Waste Management 101 (2020) 210–221

Contents lists available at ScienceDirect

Waste Management

journal homepage: www.elsevier.com/locate/wasman

Towards a circular economy: A comprehensive study of higher heat values and emission potential of various municipal solid wastes

Mehdi Bagheri [a,*], Reza Esfilar [b], Mohammad Sina Golchi [c], Christopher A. Kennedy [a]

[a] Department of Civil Engineering, University of Victoria, Victoria, British Columbia V8W 2Y2, Canada
[b] Renewable Energies and Environment Department, Faculty of New Science and Technologies, University of Tehran, Tehran, Iran
[c] Department of Engineering Science, Azad University, Science and Research Branch, Tehran, Iran

ARTICLE INFO

Article history:
Received 13 January 2019
Revised 27 September 2019
Accepted 29 September 2019

Keywords:
Municipal solid waste (MSW)
Waste-to-energy systems
High heating value (HHV)
Energy performance analysis
Circular economy

ABSTRACT

Maximizing resource recovery from waste streams (e.g., energy) is a critical challenge for municipalities. Utilizing the ultimate analysis and high heat value (HHV), we investigated the energy recovery and emission characteristics for 252 solid wastes of a diverse range of geographical origins classifications (e.g., 30 paper, 12 textile, 12 rubber and leather, 29 MSW mixture, 34 plastic, 61 wood, 20 sewage sludge and 53 other wastes) under the thermal waste-to-energy operation. Given the significance of wastes' HHV data, we proposed a rapid and cost-effective methodology for filling the gaps in the experimental data by prediction of the missing or uncertain wastes' HHV. We further employed wastes' nitrogen and sulphur contents to assess their atmospheric emissions. The results from this analysis show the highest energy content belonged to plastic waste, but higher levels of air pollution (mainly due to nitrogen and sulfur) could be emitted during thermal energy recovery of sewage sludge, rubber, and textile wastes. Also, we demonstrated more significant potential for recovering energy from plastic, wood, and paper wastes, while emitting less nitrogen and sulphur compounds to the atmosphere. Finally, our presented HHV models outperform concerning generalizability, validity, and accuracy when comparing the obtained results to those of previously published models. The results from this present study are particularly advantageous in designing sustainable thermal waste-to-energy systems to facilitate cities' transition into a circular economy.

© 2019 Elsevier Ltd. All rights reserved.

1. Introduction

As the urban population increases, the rates of resource consumption and waste generation will continue to rise. Therefore, the fast-growing use of resources and the production of municipal solid wastes (MSWs) has become a formidable challenge for public decision-makers seeking to address sustainably (Javaheri et al., 2006). MSWs are discarded materials from residential, industrial, commercial, and institutional sources that can be regarded as an opportunity instead of a burden (Rand et al., 2000). City authorities have been actively seeking sustainable waste management strategies which reduce their wastes generation while maximizing the resource recovery from wastes streams (Bagheri et al., 2018a; Koop and van Leeuwen, 2017).

Nonetheless, conventional waste management approaches (such as landfilling) has been linked to penetration and evaporation of leachates, ecological damages, infections, nuisance odors, presence of UV quenching substances in leachate and contaminated streams (Al-Khatib et al., 2015; Broun and Sattler, 2016; Iskander et al., 2018; Zhao et al., 2013). Alternatively, resource recovery from waste streams is a promising approach than the conventional waste management practices to facilitate cities' transition into a circular economy (Korhonen et al., 2018; Malinauskaite et al., 2017). In particular, waste-to-energy (WTE) technology is an attractive solution to recover renewable energy from municipal solid waste (de Souza Melaré et al., 2017; Pan et al., 2015). Not only energy recovery from urban wastes is a sustainable alternative to landfill disposal, but it also assists with the reduction of GHG emissions (Bagheri et al., 2018b; Brunner and Rechberger, 2015).

To date, a few cities have already implemented or are currently implementing WTE technologies to address the environmental and health concerns associated with urban wastes. Notably, over 2200 WTE units are estimated to operate worldwide (with an approximated capacity of 300 million tons of waste per year), while 600 additional plants are planned or currently under construction by 2025 (Bagheri et al., 2019b), resulting in a capacity of nearly 470

* Corresponding author.
E-mail address: mbagheri@uvic.ca (M. Bagheri).

https://doi.org/10.1016/j.wasman.2019.09.042
0956-053X/© 2019 Elsevier Ltd. All rights reserved.

million tons per year. Within the circular economy framework, sustainable recovery energy and materials from various waste streams has not been widely adopted by municipalities (e.g., unlike recycling and reuse programs). However, over the past few years, there has been growing interest in the adaptation of advanced WTE technologies (i.e., landfill gas recovery, thermal treatment, and biological system) by several cities around the world.

Among various WTE systems, thermal WTE systems have shown more promising given their superior techno-economic and environmental performances than their counterparts at pilot- and large-scale applications (e.g., landfill gas recovery and biological treatment) (Bagheri et al., 2019a). Accurate knowledge of the energy content and environmental impacts of the various feedstock is among the critical factors in achieving the economic and environment-friendly thermal WTE systems. While the carbon, hydrogen, and oxygen contents are beneficial for estimating the fuel's worth of wastes (Vargas-Moreno et al., 2012), information about the nitrogen and sulphur constituents are particularly valuable in evaluating the environmental (e.g., atmospheric emissions) risks associated with their thermal energy recovery (Arafat et al., 2015). Beyond the importance of elemental compositions, having precise information on the wastes' higher heating value (i.e., a proxy measure of the energy produced when waste goes through complete and partial combustion) is essential for the optimal design and operation of thermal WTE systems.

An experimental determination of HHV is a cost and time prohibitive process and requires a sophisticated experimental apparatus (i.e., bomb calorimeter) (Vargas-Moreno et al., 2012). Besides, HHV of waste feedstock changes widely and frequently throughout the WTE systems' operation, while there is no reliable real-time instrument to measure it (You et al., 2017). Hence, developing a rapid and cost-effective tool that can predict accurately the HHV of a broad range of wastes based on prior knowledge and data-mining techniques will be particularly advantageous. Favorably, utilizing the elemental composition (e.g., C, H, O, N, S, ash, and moisture) of the ultimate analysis have shown to provide the most accurate HHV estimates (Sheng and Azevedo, 2005).

Fig. 1 presents the connection between HHV evaluation and the products of thermal WTE operations. According to the various types of waste components and the complicated determination of their heat capacity in calibration experiments, predictive HHV models can save time and money. Meanwhile, HHV mathematical models evaluate the quality of wastes and can recognize how much electric power and heat energy are available in thermal treatment systems. The syngas (i.e., primarily containing hydrogen and CO) from the wastes' thermal treatment can be utilized in combined heat and power (CHP) plants to generate heat for domestic hot water and space heating and or electricity to secure the reliable power for grid-connected customers (Nami et al., 2017; Salata et al., 2017). As shown in Fig. 1, chemicals, fertilizer, and construction materials are byproducts of thermal systems and different integrated processes (e.g., composting, fuel upgrading units). Also, the produced methane from thermal WTE systems can be utilized to supply renewable transportation fuels (Ail and Dasappa, 2016). Meanwhile, other conventional fuels such as compressed natural gas (CNG), renewable natural gas (RNG), and diesel can be substituted with more sustainable alternatives (e.g., bio-CNG and bio-RNG) derived from the biomethane (Alamia et al., 2016).

Given the significance of HHV of solid wastes, several multiple regression models have been proposed to determine it from their elemental composition. For example, (Sheng and Azevedo, 2005) proposed a linear model for HHV prediction 191 biomass fuels using carbon, nitrogen, and oxygen contents, which resulted in less than ±5% estimation error for 90% of the utilized dataset. Using the carbon and hydrogen contents of biomass samples taken from previous works, (Yin, 2011) developed a two-parameter linear correlation using 44 HHV data of biomass samples taken from literature with a squared correlation coefficient (R^2) of 0.998 and an average absolute error (AAE) of less than 5%. Also, (García et al., 2014) utilized the least-squares method to report a predictive correlation for heating value of 100 different industrial waste, forestry residues, cereals, and energy crops with less than 6% absolute relative error (ARE). The complete HHV model is presented by Shi et al. (Shi et al., 2016) that included 193 MSW ultimate analysis data to develop an empirical linear HHV model using wastes' chemical constituents (e.g., C, H, O, N, S).

Despite the useful estimates, the earlier HHV models suffer from the lack of sufficient accuracy for a wide range of MSWs

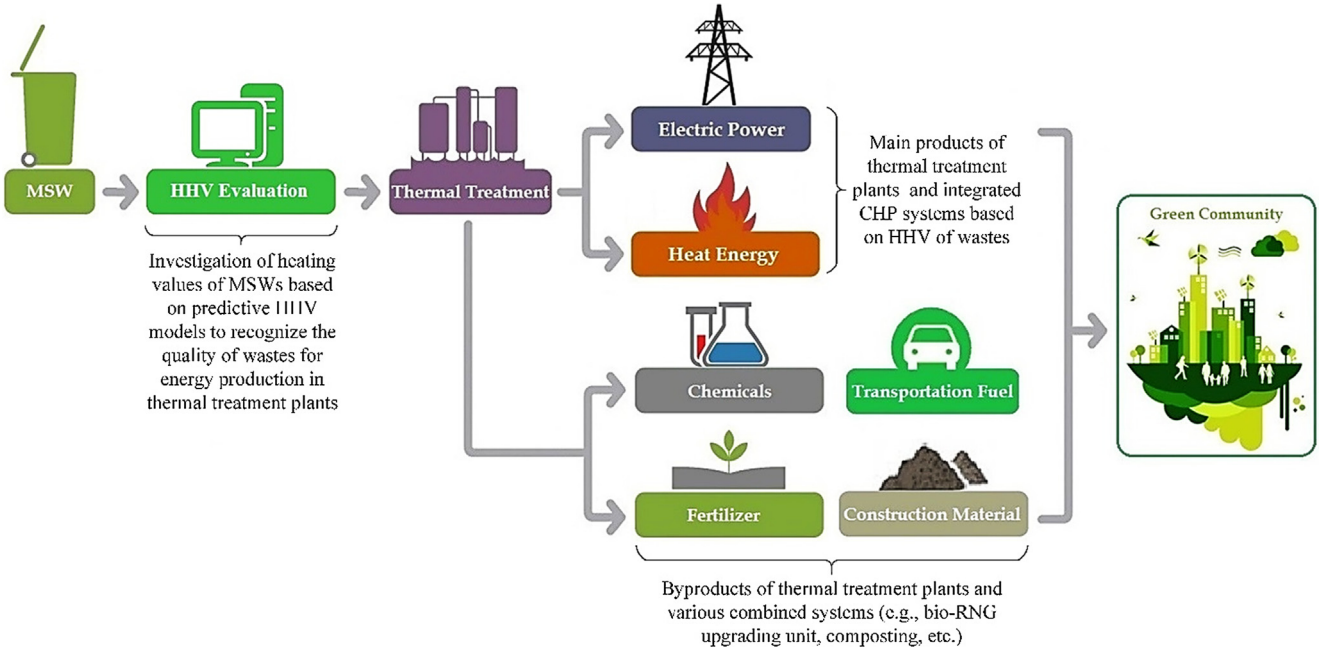

Fig. 1. Connection of heating values of MSWs and the main products of thermal waste-to-energy operations.

and waste biomass. The primary objective of this work is to investigate the potential energy content of a wide range of MSWs based on the ultimate analysis using 252 solid wastes of a diverse range of geographical origins classifications. Also, we employed wastes' nitrogen and sulphur contents to assess their atmospheric emissions. Utilizing such a comprehensive dataset, we further developed a rapid and cost-effective prediction methodology for evaluating the higher heating values of various categories of solid wastes based on a rubout dynamic binary particle swarm optimization algorithm (Bagheri et al., 2012a; Bagheri et al., 2013b). Conclusively, we compared the developed HHV models by this work with the previous studies concerning their accuracy and generalization capacities.

2. Material and methods

2.1. Dataset generation

A comprehensive list of the utilized 252 experimental HHV data by this work is available in Table A.1 (Appendix A in the Supplemental Material). The collected information includes eight different waste categories and covers a wide range of geographical sources, including 30 paper wastes, 12 textile wastes, 12 rubber/leather wastes, 29 MSWs mixture (hereafter referred to as MSWs), 34 plastic wastes, 61 wood wastes, 20 sewage sludge types and 53 other wastes. The unit of HHV in this work is MJ/kg. It is worth mentioning that the "other wastes" category is mainly composed of biomass wastes from commercial and industrial activities (e.g., coffee waste, corn stover, rice straw, kernel olive, cotton residue, urban forest residue, disposable diapers, and street sweepings).

2.2. Energy analysis

When comparing different WTE technologies, thermal-based processes benefit from a higher conversion efficiency (e.g., lower retention time) along with their capability in handling a broader range of biomass and MSWs (Thanopoulos et al., 2018). In particular, compared to the landfill gas (LFG) recovery and biological methods, the thermal WTE systems have demonstrated to emit less carbon dioxide during the partial combustion (Murphy and McKeogh, 2004) (Psomopoulos et al., 2009), reduce soil and water contaminations (McKay, 2002), while offering more valuable commercial by-products (Arena and Di Gregorio, 2013; Li et al., 2012; Zaman, 2010). Besides, the total mass and volume of residues (e.g., ash) from the thermal processes to dumpsites have been identified less than other WTE technologies (Consonni et al., 2005; Yap and Nixon, 2015).

Among various thermal WTE processes, incineration and gasification have proven the most economically feasible solutions particularly for pilot and large-scale applications (Arena, 2012; Kumar and Samadder, 2017; Psomopoulos et al., 2009). While the generated energy from incineration is the high-temperature heat, the primary energy resource from gasification is intermediate synthetic gas ($CO + H_2$) that can either be combusted for electricity production or converted into liquid fuels plus other chemical products (Baruah and Baruah, 2014; Dong et al., 2018). Nonetheless, the energy conversion efficiencies of incineration and gasification processes are directly proportional to the wastes' carbon, hydrogen, and oxygen concentration (Esfilar et al., 2018; McKendry, 2002). Likewise, their hazardous atmospheric emission (e.g., SO_X and NO_X emissions) are correlated notably with the wastes' nitrogen and sulphur compositions (Bilgen, 2014; Manahan, 2017). Therefore, to assess the energy performances for each waste categorizes under incineration and gasification operations, we respectively relied on their experimental HHV data (e.g., mainly in the form of C, H, and O) as well as the sulphur and nitrogen contents (Shi et al., 2016).

2.3. HHV modeling and validation

Given the complexities and costs of the experimental determinations of wastes' HHV, we developed a rapid and accurate HHV estimation framework for a wide range of solid wastes using an improved binary particle swarm optimization (BPSO) adopted by (Bagheri et al., 2012a). This algorithm was successfully applied and validated for developing predictive models in similar problems (Bagheri et al., 2012a; Bagheri et al., 2012b; Borhani et al., 2016) (Bagheri et al., 2013a; Bagheri et al., 2013b). Fig. 2 shows a brief description of the utilized BPSO algorithm, and a more detailed explanation of the method is provided elsewhere (Bagheri et al., 2012a).

Based on Fig. 2, the BPSO algorithm generates a population of particles based on their position (X) and velocity (V) randomly to reach an optimum condition by updating X and V using Eqs. (1)–(2):

$$V_{ij}(t+1) = wV_{ij}(t) + c_1 r_1 \left(Pbest_{ij} - X_{ij}(t)\right) + c_2 r_2 \left(Gbest_{ij} - X_{ij}(t)\right) \tag{1}$$

$$Sig(V_{ij}(t+1)) = \frac{1}{1+e^{-V_{ij}(t+1)}} \begin{cases} if & Sig(V_{ij}(t+1)) > r_3 \rightarrow X_{ij}(t+1) = 1 \\ else & X_{ij}(t+1) = 0 \end{cases} \tag{2}$$

where V_{ij} and X_{ij} represent the velocity and position of the i_{th} particle at dimension j, respectively. The parameter w is inertial weight, c_1 and c_2 are acceleration constants, and t is the iteration number. P_{best} refers to the best previous position of the i_{th} particle, G_{best} shows the global best position of all particles, and S_{ig} expresses the probability distribution of velocity based on sigmoid function. Also, r_1, r_2, and r_3 are random values in a range from 0 to 1.

The actual probabilities (P_{id}) were computed by Eq. (3), where α is a scaling factor referred to as selection pressure (Bagheri et al., 2013b). Using Eq. (3), the elements of the location vectors X_{id}^{α} and P_{id} can only take the values 0 and 1 to indicate whether the d_{th} feature is selected in the i_{th} particle (subset). To set up a subset of features comprising k members (variables), the process of spinning the wheel and selecting the feature under the wheel's marker needs to be repeated for k times. This process is repeated until a user-defined stopping criterion is reached.

$$P_{id} = \frac{X_{id}^{\alpha}}{\sum_{d=1}^{D} X_{id}^{\alpha}} \tag{3}$$

Of the most pervasive objective functions in developing data-driven models (e.g., R^2, R^2_{Adj}, Q^2, Akaike information content, and RQK function), we utilized the RQK fitness function. RQK is a multi-criteria fitness function based on the leave-one-out cross-validated variance (Q^2_{Loo} statistics, presented by Eq. (4):

$$Q^2_{LOO} = 1 - \frac{\sum_{i=1}^{n} (HHV_i - HHV_{ic})^2}{\sum_{i=1}^{n} (HHV_i - \overline{HHV})^2} \tag{4}$$

where n is the number of data in the training set, HHV_i is the experimental high heat value for the i_{th} waste of the training set, HHV_{ic} is the predicted high heat value of i_{th} waste by a model obtained with this waste excluded, and $\overline{HHV}$ is the mean of the high heat value for all wastes in the training set. (Todeschini et al., 2004) showed that the data-driven models obtained by the RQK function when satisfying the four following constraints (Eqs. (5)–(8)) possess a higher accuracy and prediction power than the other fitness functions.

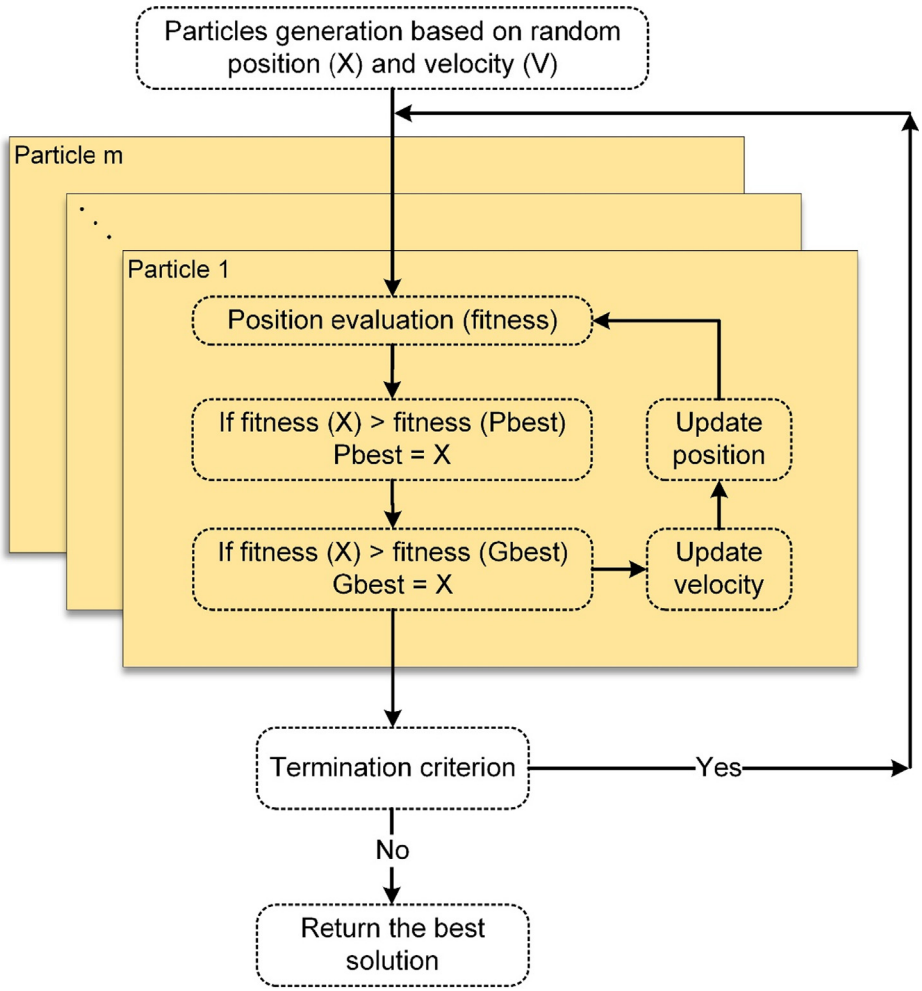

Fig. 2. Flowchart of the utilized BPSO method.

$$\Delta K = K_{xy} - K_x > 0(QUIK\ \ rule) \tag{5}$$

$$\Delta Q = Q^2_{LOO} - Q^2_{ASYM} > 0\left(Asymptotic\ \ Q^2\ \ rule\right) \tag{6}$$

$$R^P > 0(Redundancy\ \ RP\ \ rule) \tag{7}$$

$$R^N > 0(Overfitting\ \ RN\ \ rule) \tag{8}$$

For this work, we utilized the RQK fitness function in the model evolution of the BPSO algorithm. Before executing the algorithm mentioned above, we randomly divided the original dataset into training and test sub-datasets. As an example, 85% of the data set was used for training and the remaining 15% for the test set. Finally, the proposed BPSO algorithm was coded in MATLAB v16b (Mathworks Inc.) (MATLAB, 2016), with the total execution time of about 30 min using a Windows 7 platform of personal computer with an Intel(R) Core(TM) i7, CPU@2.50 GHz, 12 GB RAM.

3. Results and discussion

3.1. Energy and emission performances

Table 1 presents the lower and upper bounds of the HHV data and the elemental components of the eight waste categories used in this study. As shown in Table 1, the carbon contents vary significantly between and across different waste classes. Overall, the highest carbon composition respectively belongs to plastic, rubber/leather, textile, and MSW mixture followed by wood and paper wastes. Similarly, sewage sludge, rubber/leather, and plastic wastes emit more air pollutants due to their higher sulphur and nitrogen concentrations when compared to other classifications.

To gain further understanding of the energy and emission performance of the eight categories, Fig. 3a presents the average HHV values for different wastes. According to Fig. 3a, plastics have the greatest HHV when compared to other groups. Rubbers/leathers and textiles are in the second and third place regarding their average HHV data. On the contrary, the lowest average HHV belongs to sewage sludge that is almost four times less than plastics. Based on Fig. 3a, wood, paper, MSW mixture, and other wastes demonstrate a relatively similar average HHV. To compare the emission performance of various waste categories, Fig. 3b illustrates the average values of sulphur and nitrogen contents. Based on Fig. 3b, sewage sludge, rubber/leather, and textile wastes have higher average nitrogen concentration. However, sewage sludge shows almost 50% greater nitrogen content compared to textile and rubber/leather wastes. Nonetheless, sewage sludge and rubber/leather wastes behave very similarly concerning the average concentration of sulphur constitute.

To gain further insights into the energy performance of various wastes, we will discuss the variability of elemental compositions and develop HHV models for each of the waste categories used in this work.

Table 1
Statistical variability of ultimate analysis and high heating values utilized in this work.

Category	Ultimate analysis										HHV (MJ/kg)	
	C		H		O		N		S			
	min	max	min	max	min	max	min	max	min	max	min	max
Paper	30.5	59.2	3.5	9.3	27.5	47.8	0.0	2.9	0.0	1.5	10.4	27.3
Textile	46.2	66.9	4.3	9.7	2.0	43.6	0.1	5.5	0.0	0.7	18.7	31.2
Rubber/ leather	42.0	84.8	5.2	9.4	2.7	23.2	0.0	10.0	0.0	2.5	19.7	38.0
MSW Mixture	31.2	59.2	3.8	0.1	21.8	39.8	0.2	3.3	0.0	0.8	12.0	27.6
Plastic	38.0	92.0	4.9	14.5	0.0	44.8	0.0	6.0	0.0	2.6	19.2	49.3
Wood	36.2	53.8	4.8	8.8	26.6	47.7	0.0	7.0	0.0	1.2	14.6	23.3
Other wastes	20.6	56.1	2.9	7.6	4.0	48.6	0.0	6.3	0.0	1.2	9.1	22.6
Sewage sludge	9.0	31.1	2.0	4.6	15.7	27.5	1.5	5.0	0.4	2.0	3.5	13.9

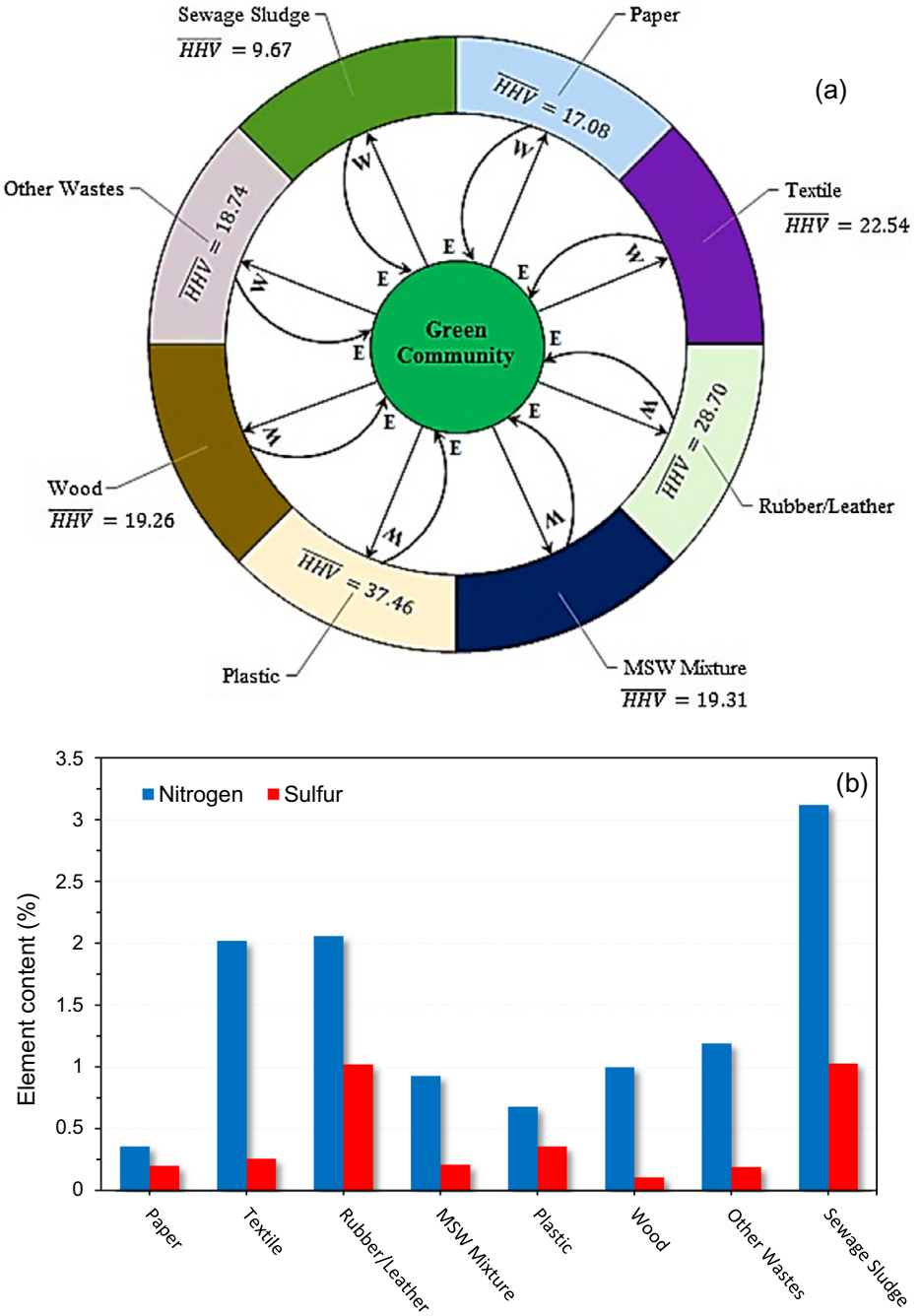

Fig. 3. (a) Average HHV values, and (b) average nitrogen and sulfur content for the eight different waste categories.

3.1.1. Paper

Fig. 4a illustrates the variability across the elemental composition and experimental HHV for various paper wastes used for this study. While the average HHV of paper wastes for energy production is 17.1 MJ/kg., coated and glossy papers are potentially the highest SOx and NOx emitters of this waste category (e.g., due to their higher sulphur and nitrogen contents). According to Fig. 4a, magazines, coated and glossy papers have the least carbon constitutes and HHV data compared to other paper wastes. Meanwhile, cartons (particularly waxed milk type) and newspapers have higher carbon and hydrogen contents, therefore having more significant energy content than the other paper wastes (see Fig. 4a). Eq. (9) presents the HHV model obtained from the BPSO algorithm. Based on Eq. (9), the most critical factors in the energy performance of paper wastes are the carbon and hydrogen contents.

Fig. 5a displays the predicted values of HHV (Eq. (9)) in comparison to the experimental data. Based on Fig. 5a, there are only very few paper wastes with more than 5% estimation errors. However, the overestimation of HHV data for magazines and coated papers might be mainly due to coating (impurities) materials, which often reduces the energy performance of the paper wastes. Also, in the case of large model prediction error values for magazines and coated papers, more reliable experimental data would be particularly advantageous to judge the model capability better.

$$HHV_{Paper} = 20.14 + (9.00 \times 10^{-7})C^4 - (37.25)\frac{1}{H} \quad (9)$$

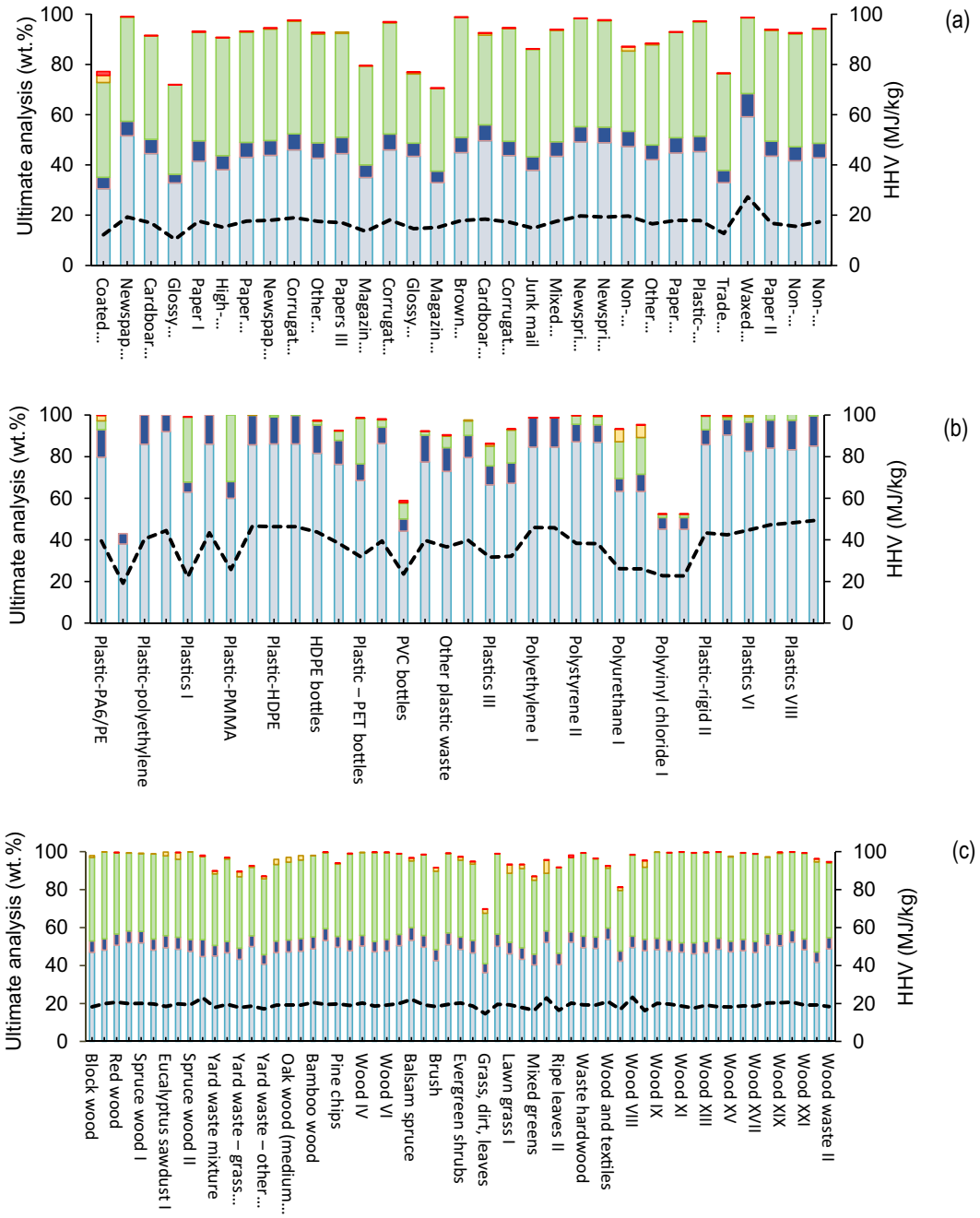

Fig. 4. Energy content and experimental HHV trend for each waste category based on ultimate analysis, (a) papers, (b) plastics, (c) wood residues, (d) MSW mixtures, (e) rubbers/leathers, (f) textiles, (g) sewage sludge, (h) other different wastes.

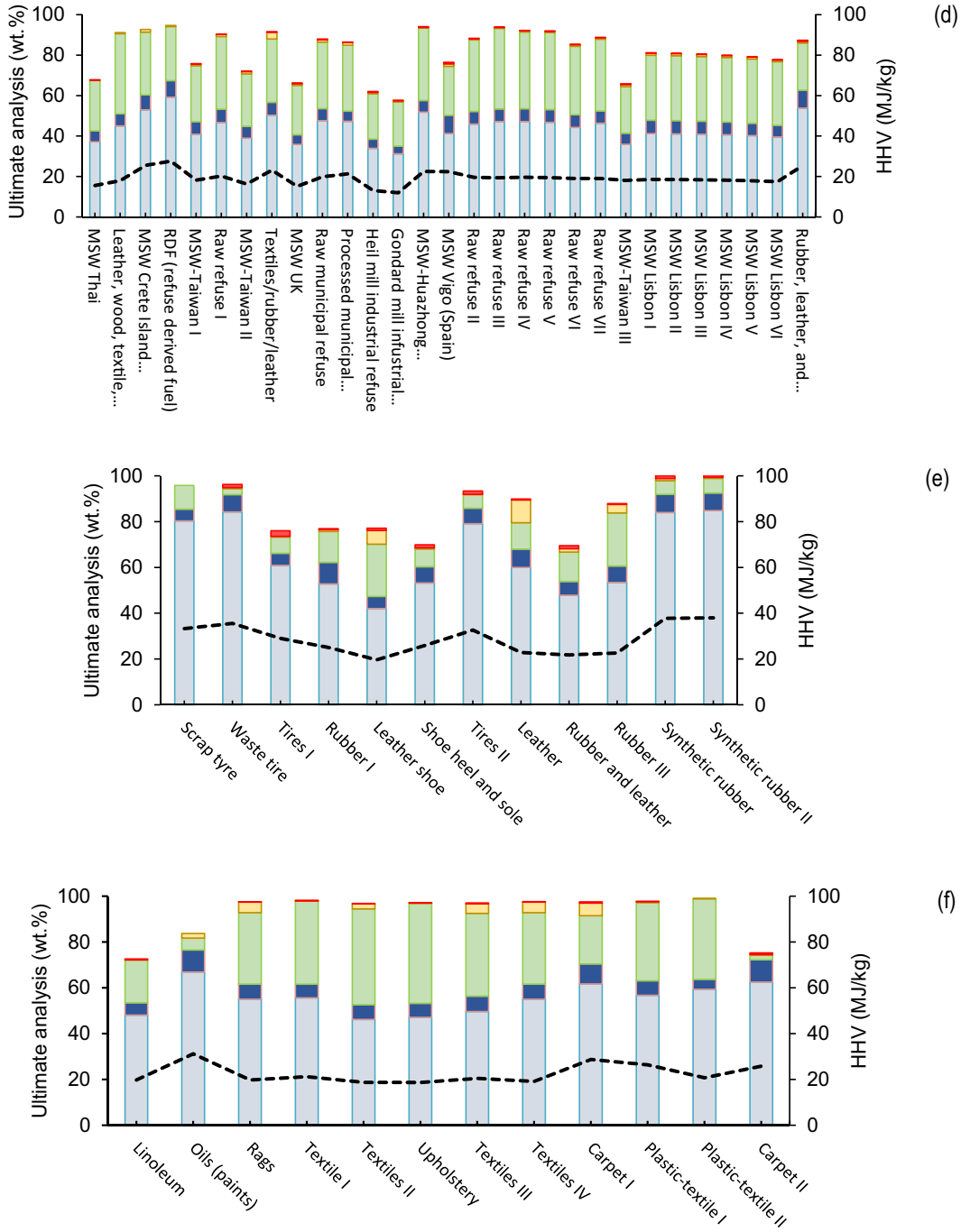

Fig. 4 (*continued*)

$n = 31, R^2 = 93.76, R^2_{adj} = 93.32, Q^2_{Loo} = 92.68, Q^2_{Boot} = 91.40, RMSE = 0.772, AARE\% = 3.50$

RQK function parameters: $\Delta K = 0.138$, $\Delta Q = 0.003, R^P = 0.040, R^N = 0.001$

It is worth mentioning that given the limited size of test data for the three categories of "rubber and leather", "textile", "and "sewage sludge", we utilized the cross-validation approach to assessing the prediction performance of the HHV models. In other words, we developed several models using different training and test sets to ensure less than 5% variation in the error estimations and statistical indicators for the reported HHV models.

3.1.2. Plastic

Fig. 4b depicts the elemental analysis and energy output of plastics. The average percentage of carbon, hydrogen, and oxygen composition is 95.38%, and that of nitrogen and sulphur are very low. However, the polyurethanes disperse hazardous material in the air after combustion. The plastic (IX) produces remarkable energy in comparison to other plastics. HDPE and LDPE have high energy content and acceptable environmental impacts. The results indicate that the most important for energy content is carbon composition. For instance, the energy content of HDPE and plastic-PP is equal due to the same carbon content. It should be considered the sum of hydrogen and oxygen compositions of these two plastics are different. Generally, the average HHV of obtained around

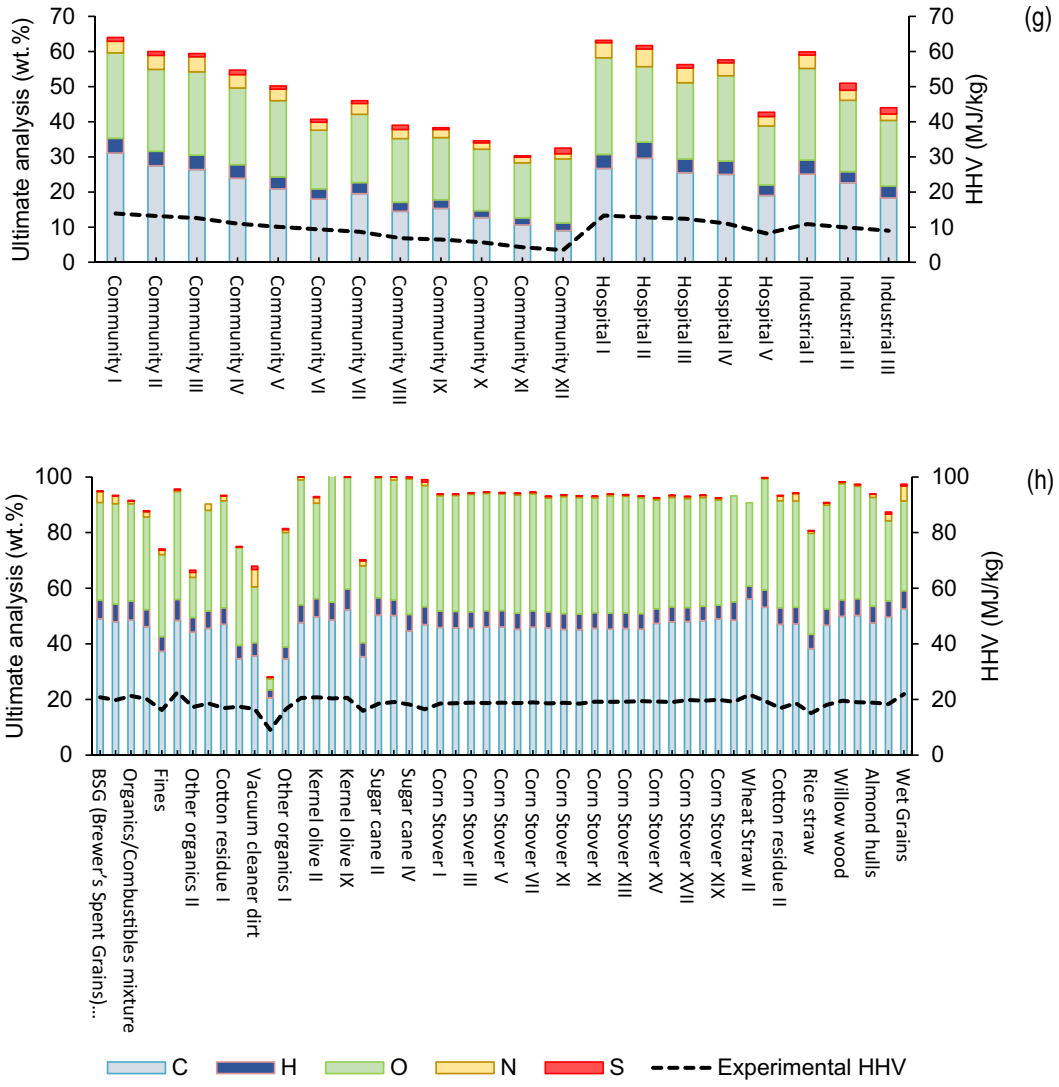

Fig. 4 (*continued*)

37.46 MJ/kg for plastics, which is higher than the heating value of other waste categories. Fig. 5b (along with the statistics presented following Eq. (10)) demonstrates that carbon and hydrogen contents are two essential parameters for the HHV calculation of plastic wastes. The double-input HHV model of plastics presents that waste with higher carbon and hydrogen contents will have higher HHV.

$$HHV_{Plastic} = 13.112 + 0.003C^2 + 0.051H^2 \quad (10)$$

$n = 34$, $R^2 = 94.07$, $R^2_{adj} = 93.69$, $Q^2_{Loo} = 92.78$, $Q^2_{Boot} = 92.71$, $RMSE = 2.162$, $AARE\% = 4.77$

RQK function parameters: $\Delta K = 0.174$, $\Delta Q = -0.001$, $R^P = 0.036$, $R^N = 0.00$

3.1.3. Wood

Wood wastes' elemental compositions along with the experimental HHV values are shown in Fig. 4c. According to Fig. 4c, wood (VIII), wood (I), and ripe leaves (I) have more significant energy recovery potential than other wood wastes in combustion units. Although the average of C, H, and O compositions of wood wastes (95.30%) is equal to the values of plastics approximately, the mean heating value (19.26 MJ/kg) and energy content of woods are lower than plastics under thermal WTE treatment. In this category, ripe leaves, lawn grasses, yard wastes, and fiberboards are expected to emit higher concentrations of nitrogenous and sulphurous pollutants into the air.

Eq. (11) presents the obtained BPSO model for the wood wastes used in this work. According to the coefficients of Eq. (11), the effect of carbon contents is higher than hydrogen and nitrogen. Thus, wood wastes with higher carbon contents will potentially generate more energy during their thermal recovery. A comparison of the experimental HHV and predicted values for the training and test sets are displayed graphically in Fig. 5c. This figure indicates that training and test sets are dispersed well between the problem searching space, and the model external test prediction statistics are analogous to the training statistics.

$$HHV_{Wood} = 4.786 + 0.290C + 10^{-5}H^6 + (2 \times 10^{-5})N^6 \quad (11)$$

$n = 61$, $R^2 = 68.64$, $R^2_{adj} = 66.99$, $Q^2_{Loo} = 65.85$, $Q^2_{Boot} = 0.00$, $RMSE = 0.855$, $AARE\% = 3.08$

RQK function parameters: $\Delta K = 0.241$, $\Delta Q = 0.018$, $R^P = 0.171$, $R^N = 0.00$

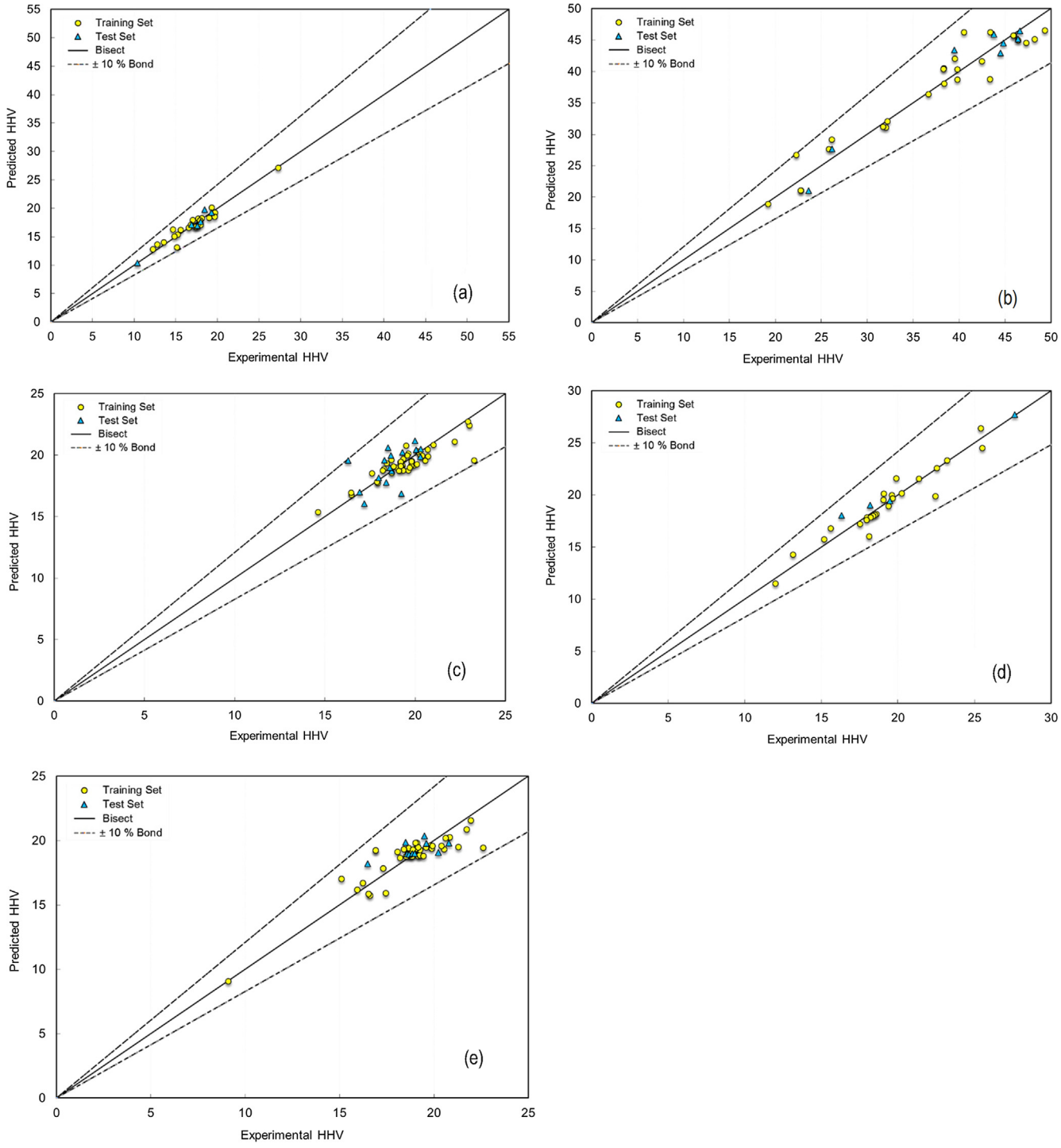

Fig. 5. Comparison of experimental and predicted HHV for each waste category, (a) papers, (b) plastics, (c) wood residues, (d) MSW mixtures, (e) other different wastes.

3.1.4. MSW mixture

Fig. 4d exhibits the experimental HHV along with the associated elemental compositions for waste mixtures. As shown in Fig. 4d, the highest energy content belongs to refuse-derived fuels (RDFs) with around 95% carbon, hydrogen, and oxygen composition. After RDFs, the mixture of MSW and hard plastics benefits from a higher energy content than other waste mixtures. Also, the average heating value of the MSW mixtures calculated about 19.3 MJ/kg. Based on Fig. 4d, there is a distinct incremental positive relationship between the waste mixtures' HHV and their carbon contents. Accordingly, mixtures of rubber, leather, and textile wastes are supposed to emit higher atmospheric pollutants than other waste mixtures due to their greater concentrations of sulphur and nitrogen (e.g., on average about 1.14%). We presented the HHV BPSO model of waste mixtures in Eq. (12). A comparison of experimental and predicted data demonstrates an acceptable accuracy in estimating the HHV data for a majority of waste mixtures (Fig. 5d).

$$HHV_{Mixture} = 48.373 - 1120.66\frac{1}{C} - 0.0001O^3 \quad (12)$$

$n = 29$, $R^2 = 92.62$, $R^2_{adj} = 92.05$, $Q^2_{Loo} = 90.87$, $Q^2_{Boot} = 90.77$, $RMSE = 0.917$, $AARE\% = 3.68$

RQK function parameters: $\Delta K = 0.029$, $\Delta Q = 0.00$, $R^P = 0.147$, $R^N = -0.334$

3.1.5. Rubber and leather

Fig. 4e shows the extent of variations across different rubber and leather wastes used in this work. Based on Fig. 4e, the highest potential for energy recovery belongs to the synthetic rubbers, waste tires, and scrap tire that have a relatively high C, H, and O contents (e.g., about 90%). The calculated average of HHV for rubber and leather wastes is almost 28.7 MJ/kg. Also, the heat values of this category of wastes showed to have a negative correlation with their oxygen content. However, leather and rubber wastes showed to cause more significant hazardous air pollutants because of their relatively higher nitrogen and sulphur concentrations.

By executing the BPSO algorithm, we developed the following HHV for rubber and leather wastes (Eq. (13)). According to Eq. (13), carbon and nitrogen are the key factors influencing the heat recovery potential of rubber and leather wastes. Based on the coefficient signs (see Eq. (13)) for the nitrogen and carbon, rubbers/leathers with lower nitrogen and higher carbon contents will create more energy from their thermal decomposition.

$$HHV_{Rubber} = 11.578 + 0.067\sqrt[3]{C^4} - 0.210\sqrt[3]{N^4} \quad (13)$$

$n = 12$, $R^2 = 96.38$, $R^2_{adj} = 95.58$, $Q^2_{Loo} = 94.53$, $Q^2_{Boot} = 73.57$, $RMSE = 1.196$, $AARE\% = 3.64$

RQK function parameters: $\Delta K = 0.264$, $\Delta Q = 0.010$, $R^P = 0.034$, $R^N = 0.00$

3.1.6. Textile

Fig. 4f presents the changes in elemental compositions and the experimental HHV data for the textile waste category. Subsequently, the average HHV for textile wastes calculated 22.5 MJ/kg, which is almost 24% higher than the paper wastes. Based on Fig. 4f, the trends of HHV data is well consistent with the changes in the carbon content. As for the energy recovery potentials, petroleum-based manufactured fibers and carpet (e.g., acrylic, polyester, and nylon) had the highest carbon contents and HHV data when compared to the other textile wastes. While textile wastes with more wool, nylon, and or polyester materials have more nitrogen contents, cotton products (fabrics) tend to have higher sulphur contents, e.g., mainly due to the high volume of sulphur dyes during their processing (see Eq. (14)).

$$HHV_{textile} = 600.1 - 336.9\sqrt{C} + 132.76\sqrt[3]{C^2} \quad (14)$$

$n = 12$, $R^2 = 84.35$, $R^2_{adj} = 80.88$, $Q^2_{Loo} = 76.90$, $Q^2_{Boot} = 73.15$, $RMSE = 1.629$, $AARE\% = 7.41$

RQK function parameters: $\Delta K = 0.014$, $\Delta Q = 0.047$, $R^P = 0.04$, $R^N = 0.00$

3.1.7. Sewage sludge

As shown in Fig. 4g, carbon composition plays a crucial role in identifying the HHV of sewage sludge. We calculated the average HHV of 9.7 MJ/k for the sewage sludge that is mainly due to the lower contents of carbon, hydrogen, and oxygen in this waste category. Nonetheless, the average contents of nitrogen and sulphur were higher than other waste categories that might cause more significant environmental concerns over the use of sewage sludge for the thermal energy recovery. Eq. (15) predicts HHV obtained from the BPSO model, which shows less than 5% estimation error for the majority of data in this category.

$$HHV_{Sludge} = -4.40 + 1.79\sqrt[3]{C^2} + (161.00 \times 10^{-5})O^2 \quad (15)$$

$n = 20$, $R^2 = 98.06$, $R^2_{adj} = 97.70$, $Q^2_{Loo} = 96.51$, $Q^2_{Boot} = 96.53$, $RMSE = 0.416$, $AARE\% = 5.51$

RQK function parameters: $\Delta K = -0.003$, $\Delta Q = -0.005$, $R^P = 0.001$, $R^N = 0.00$

3.1.8. Others

Fig. 4h presents characteristics of various wastes such as organic materials, fines, household waste, and agricultural residues. In this category, disposable diapers showed the highest energy outputs and as well as nitrogen and sulphur contents. Grains, wheat straw, kernel olives, corn stover, and willow wood also identifies with higher energy contents than the other agricultural wastes. Also, the combustion of wet grains, BSG waste, and coffee wastes possess higher emission risks due to higher nitrogen and sulphur oxide gases due to the greater N and S contents in their chemical composition. The developed Eq. (16) for this waste category showed to provide an accurate HHV estimate for coffee waste, fines, corn stover, household dirt, and other organic mixtures. Also, the negative coefficient of sulphur in this equation reveals a negative correlation between the HHV data and the sulphur content. On the contrary, the concentrations of nitrogen and carbon showed to have a positive relationship with the HHV data. Fig. 5e represents the distribution of training and test sets when compared to the experimental HHV data for the other wastes.

$$HHV_{Other} = 39.004 - 135.829\frac{1}{\sqrt{C}} - 1.816S^4 + 0.011N^3 \quad (16)$$

$n = 53$, $R^2 = 82.77$, $R^2_{adj} = 81.71$, $Q^2_{Loo} = 81.32$, $Q^2_{Boot} = 76.03$, $RMSE = 0.837$, $AARE\% = 3.75$

RQK function parameters: $\Delta K = 0.208$, $\Delta Q = 0.015$, $R^P = 0.056$, $R^N = -0.403$

3.2. Model verification

To validate the proposed HHV models, their accuracy should be checked autonomously by similar reference data. Table 2 compares the statistical analysis of our proposed models against the previous HHV studies (Shi et al., 2016; Thipkhunthod et al., 2005). Among the most widely-applied analytical measures to assess the statistical performance of data-driven models, we utilized: coefficient of determination (R^2), adjusted coefficient of determination (R^2_{adj}), root mean square error (*RMSE*), and average absolute error (*AAE*). Formally, when the RMSE is at the minimum, and R^2 is high (e.g., higher than 0.7), a model can be considered as very good (Bagheri et al. 2013a). Besides, it is important that RMSE values for the training and test sets are not only low but also very similar, which suggests that the model has both predictive ability (low values) and generalization performance (similar values). Meanwhile, to further assess the model validity, we employed additional statistical tests such as y-scrambling, bootstrap, and external validation techniques. As shown by the analytical results, the small differences between R^2, Q^2_{Boot}, and Q^2_{Loo} demonstrate that the model has an excellent prediction performance (Bagheri et al., 2012b; Bozorgi et al., 2013).

According to Table 2, the results show an acceptable high accuracy of the proposed HHV models by this study. Based on Table 2 (e.g., R^2, R^2_{Adj}, RSME, AAE), our proposed HHV models perform better than the previous work concerning their generalizability, validity, and accuracy. In particular, the *RMSE*s for all waste categories including papers (0.772), woods (0.855), MSWs (0.917), rubbers/leathers (1.196), and other organic wastes (0.837) are significantly less than

Table 2
Statistical performance of the developed HHV models with the previous works (Shi et al., 2016; Thipkhunthod et al., 2005).

References	Dataset Size	No. of inputs	R^2	R^2_{adj}	RMSE	AAE	Applications
This work							
Eq. (9)	31	2	0.938	0.933	0.772	0.02	*Paper*
Eq. (10)	34	2	0.941	0.937	2.162	0.05	*Plastic*
Eq. (11)	61	3	0.686	0.670	0.855	0.01	*Wood*
Eq. (12)	29	2	0.926	0.909	0.917	0.02	*MSW mixture*
Eq. (13)	12	2	0.964	0.956	1.196	0.09	*Rubber & leather*
Eq. (14)	12	1	0.843	0.809	1.629	0.14	*Textile*
Eq. (15)	12	2	0.981	0.977	0.416	0.02	*Sewage sludge*
Eq. (16)	53	3	0.828	0.817	0.837	0.01	*other wastes*
Previous works							
Shi et al. (2016)	193	3	0.949	0.948	2.02	1.35	*Wood, paper, rubber, textile, plastic*
Shi et al. (2016)	193	4	0.961	0.960	1.70	1.13	*Wood, paper, rubber, textile, plastic*
Shi et al. (2016)	193	5	0.966	0.966	1.54	1.09	*Wood, paper, rubber, textile, plastic*
Thipkhunthod et al. (2005)	30	5	0.650	0.649	5.47	4.65	*Sewage sludge*

* RMSE: root-mean-square error, R^2_{adj}: adjusted correlation coefficient, AAE: average absolute error

Table 3
Correlation matrix of the model variables and HHV data.

	Carbon	Hydrogen	Oxygen	Nitrogen	Sulphur	HHV
Carbon	1.00	–	–	–	–	–
Hydrogen	0.82	1.00	–	–	–	–
Oxygen	−0.07	0.00	1.00	–	–	–
Nitrogen	−0.38	−0.36	−0.25	1.00	–	–
Sulfur	−0.24	−0.17	0.29	−0.14	1.00	–
HHV	0.95	0.89	0.06	−0.49	−0.21	1.00

the three HHV models proposed by Shi et al. (Shi et al., 2016). Finally, it is worth mentioning that our models require fewer inputs (variables) for the HHV estimation when compared to the previous studies. Since the experimental quantification of trace elemental compositions is both cost and time prohibitive, the application of our models is particularly advantageous because of offering a more accurate HHV estimate with less information and at a lower price.

Table 3 shows the correlation matrix between all the variables of the ultimate analysis. The results demonstrate that the highest negative correlation occurs between HHV (energy content) and nitrogen content (−0.49). Also, the lowest correlation belongs to HHV and oxygen (0.06), which means oxygen content has the lowest impact on energy content. The highest positive correlations appear between HHV and carbon (0.95), HHV and hydrogen (0.89), carbon and hydrogen (0.82), respectively. Consequently, in general, with increasing the C, H, and O, the heating value of fuels increase approximately.

4. Conclusions

This paper investigated the potentials of energy recovery from various municipal wastes (e.g., including papers, textiles, rubbers, plastics, mixtures, woods, sewage sludge, and others) under thermal WTE operation. Also, we employed wastes' nitrogen and sulphur contents to assess their atmospheric emissions. Using a robust BPSO algorithm, we further developed a user-friendly and inexpensive method to provide waste practitioners and researchers with accurate yet straightforward HHV estimates for a wide range of waste categories. The results from this analysis show that plastic wastes showed the highest energy outputs under thermal WTE systems owned to their higher HHV mean value (37.46 MJ/kg). Using sewage sludge, rubbers, leathers, and textiles might pose more risks to the environment (e.g., mainly concerning hazardous atmospheric emissions) due to their higher concentrations of nitrogen and sulphur. In this context, when considering a higher energy recovery along with lower sulphur and nitrogen contents; plastics, woods, papers, and agricultural residues are a more appropriate feedstock for the thermal WTE systems. When compared to the previous models, our presented HHV models outperform concerning generalizability, validity, and accuracy when comparing the obtained results to those of previously published models. Therefore, they can be relied on to fill the gaps in the experimental data by prediction of the missing or uncertain wastes' HHV.

Appendix A. Supplementary material

Supplementary data to this article can be found online at https://doi.org/10.1016/j.wasman.2019.09.042.

References

Ail, S.S., Dasappa, S., 2016. Biomass to liquid transportation fuel via Fischer Tropsch synthesis technology review and current scenario. Renew. Sustain. Energy Rev. 58, 267–286.
Al-Khatib, I.A., Kontogianni, S., Nabaa, H.A., Al-Sari, M.I., 2015. Public perception of hazardousness caused by current trends of municipal solid waste management. Waste Manage. 36, 323–330.
Alamia, A., Magnusson, I., Johnsson, F., Thunman, H., 2016. Well-to-wheel analysis of bio-methane via gasification, in heavy-duty engines within the transport sector of the European Union. Appl. Energy 170, 445–454.
Arafat, H.A., Jijakli, K., Ahsan, A., 2015. Environmental performance and energy recovery potential of five processes for municipal solid waste treatment. J. Cleaner Prod. 105, 233–240.
Arena, U., 2012. Process and technological aspects of municipal solid waste gasification. A review. Waste Manage. 32, 625–639.
Arena, U., Di Gregorio, F., 2013. Element partitioning in combustion- and gasification-based waste-to-energy units. Waste Manage. 33, 1142–1150.
Bagheri, M., Alivand, M.S., Alikarami, M., Kennedy, C.A., Doluweera, G., Guevara, Z., 2019a. Developing a multiple-criteria decision analysis for green economy transition: a Canadian case study. Econ. Syst. Res., 1–25
Bagheri, M., Borhani, T.N.G., Zahedi, G., 2012a. Estimation of flash point and autoignition temperature of organic sulfur chemicals. Energy Convers. Manage. 58, 185–196.
Bagheri, M., Borhani, T.N.G., Zahedi, G., 2013a. Simple yet accurate prediction of liquid molar volume via their molecular structure. Fluid Phase Equilib. 337, 183–190.
Bagheri, M., Delbari, S.H., Pakzadmanesh, M., Kennedy, C.A., 2019b. City-integrated renewable energy design for low-carbon and climate-resilient communities. Appl. Energy 239, 1212–1225.

Bagheri, M., Guevara, Z., Alikarami, M., Kennedy, C.A., Doluweera, G., 2018a. Green growth planning: A multi-factor energy input-output analysis of the Canadian economy. Energy Econ. 74, 708–720.
Bagheri, M., Rajabi, M., Mirbagheri, M., Amin, M., 2012b. BPSO-MLR and ANFIS based modeling of lower flammability limit. J. Loss Prev. Process Ind. 25, 373–382.
Bagheri, M., Shirzadi, N., Bazdar, E., Kennedy, C.A., 2018b. Optimal planning of hybrid renewable energy infrastructure for urban sustainability: Green Vancouver. Renew. Sustain. Energy Rev. 95, 254–264.
Bagheri, M., Yerramsetty, K., Gasem, K.A., Neely, B.J., 2013b. Molecular modeling of the standard state heat of formation. Energy Convers. Manage. 65, 587–596.
Baruah, D., Baruah, D., 2014. Modeling of biomass gasification: a review. Renew. Sustain. Energy Rev. 39, 806–815.
Bilgen, S., 2014. Structure and environmental impact of global energy consumption. Renew. Sustain. Energy Rev. 38, 890–902.
Borhani, T.N.G., Saniedanesh, M., Bagheri, M., Lim, J.S., 2016. QSPR prediction of the hydroxyl radical rate constant of water contaminants. Water Res. 98, 344–353.
Broun, R., Sattler, M., 2016. A comparison of greenhouse gas emissions and potential electricity recovery from conventional and bioreactor landfills. J. Cleaner Prod. 112, 2664–2673.
Brunner, P.H., Rechberger, H., 2015. Waste to energy key element for sustainable waste management. Waste Manage. 37, 3–12.
Consonni, S., Giugliano, M., Grosso, M., 2005. Alternative strategies for energy recovery from municipal solid waste: Part B: Emission and cost estimates. Waste Manage. 25, 137–148.
de Souza Melaré, A.V., González, S.M., Faceli, K., Casadei, V., 2017. Technologies and decision support systems to aid solid-waste management: a systematic review. Waste Manage. 59, 567–584.
Dong, J., Tang, Y., Nzihou, A., Chi, Y., Weiss-Hortala, E., Ni, M., 2018. Life cycle assessment of pyrolysis, gasification and incineration waste-to-energy technologies: Theoretical analysis and case study of commercial plants. Sci. Total Environ. 626, 744–753.
Esfilar, R., Mehrpooya, M., Moosavian, S.A., 2018. Thermodynamic assessment of an integrated biomass and coal co-gasification, cryogenic air separation unit with power generation cycles based on LNG vaporization. Energy Convers. Manage. 157, 438–451.
García, R., Pizarro, C., Lavín, A.G., Bueno, J.L., 2014. Spanish biofuels heating value estimation. Part I: Ultimate analysis data. Fuel 117, 1130–1138.
Iskander, S.M., Zhao, R., Pathak, A., Gupta, A., Pruden, A., Novak, J.T., He, Z., 2018. A review of landfill leachate induced ultraviolet quenching substances: Sources, characteristics, and treatment. Water Res. 145, 297–311.
Javaheri, H., Nasrabadi, T., Jafarian, M., Rowshan, G., Khoshnam, H., 2006. Site selection of municipal solid waste landfills using analytical hierarchy process method in a geographical information technology environment in Giroft. J. Environ. Health Sci. Eng. 3, 177–184.
Koop, S.H., van Leeuwen, C.J., 2017. The challenges of water, waste and climate change in cities. Environ. Dev. Sustain. 19, 385–418.
Korhonen, J., Honkasalo, A., Seppälä, J., 2018. Circular economy: the concept and its limitations. Ecol. Econ. 143, 37–46.
Kumar, A., Samadder, S., 2017. A review on technological options of waste to energy for effective management of municipal solid waste. Waste Manage. 69, 407–422.
Li, X.-G., Lv, Y., Ma, B.-G., Chen, Q.-B., Yin, X.-B., Jian, S.-W., 2012. Utilization of municipal solid waste incineration bottom ash in blended cement. J. Cleaner Prod. 32, 96–100.
Malinauskaite, J., Jouhara, H., Czajczyńska, D., Stanchev, P., Katsou, E., Rostkowski, P., Thorne, R.J., Colón, J., Ponsá, S., Al-Mansour, F., 2017. Municipal solid waste management and waste to energy in the context of a circular economy and energy recycling in Europe. Energy 141, 2013–2044.
Manahan, S., 2017. Environmental Chemistry. CRC Press, Boca Raton.
MATLAB, 2016. The Mathworks Inc. Novi, Michigan.
McKay, G., 2002. Dioxin characterization, formation and minimization during municipal solid waste (MSW) incineration. Chem. Eng. J. 86, 343–368.
McKendry, P., 2002. Energy production from biomass (part 1): overview of biomass. Bioresour. Technol. 83, 37–46.
Murphy, J.D., McKeogh, E., 2004. Technical, economic and environmental analysis of energy production from municipal solid waste. Renew. Energy 29, 1043–1057.
Nami, H., Mahmoudi, S., Nemati, A., 2017. Exergy, economic and environmental impact assessment and optimization of a novel cogeneration system including a gas turbine, a supercritical CO_2 and an organic Rankine cycle (GT-HRSG/SCO2). Appl. Therm. Eng. 110, 1315–1330.
Pan, S.-Y., Du, M.A., Huang, I.-T., Liu, I.-H., Chang, E., Chiang, P.-C., 2015. Strategies on implementation of waste to energy (WTE) supply chain for circular economy system: a review. J. Cleaner Prod. 108, 409–421.
Psomopoulos, C., Bourka, A., Themelis, N.J., 2009. Waste to energy: A review of the status and benefits in the USA. Waste Manage. 29, 1718–1724.
Rand, T., Haukohl, J., Marxen, U., 2000. Municipal solid waste incineration: requirements for a successful project (English), Washington, D.C., p. 118.
Salata, F., Golasi, I., Domestico, U., Banditelli, M., Basso, G.L., Nastasi, B., de Lieto Vollaro, A., 2017. Heading towards the nZEB through CHP+ HP systems. A comparison between retrofit solutions able to increase the energy performance for the heating and domestic hot water production in residential buildings. Energy Convers. Manage. 138, 61–76.
Sheng, C., Azevedo, J., 2005. Estimating the higher heating value of biomass fuels from basic analysis data. Biomass Bioenergy 28, 499–507.
Shi, H., Mahinpey, N., Aqsha, A., Silbermann, R., 2016. Characterization, thermochemical conversion studies, and heating value modeling of municipal solid waste. Waste Manage. 48, 34–47.
Thanopoulos, S., Karellas, S., Kavrakos, M., Konstantellos, G., Tzempelikos, D., Kourkoumpas, D., 2018. Analysis of alternative MSW treatment technologies with the aim of energy recovery in the municipality of vari-voula-vouliagmeni. Waste Biomass Valorization, 1–17.
Thipkhunthod, P., Meeyoo, V., Rangsunvigit, P., Kitiyanan, B., Siemanond, K., Rirksomboon, T., 2005. Predicting the heating value of sewage sludges in Thailand from proximate and ultimate analyses. Fuel 84, 849–857.
Todeschini, R., Consonni, V., Mauri, A., Pavan, M., 2004. Detecting "bad" regression models: multicriteria fitness functions in regression analysis. Anal. Chim. Acta 515, 199–208.
Vargas-Moreno, J., Callejón-Ferre, A., Pérez-Alonso, J., Velázquez-Martí, B., 2012. A review of the mathematical models for predicting the heating value of biomass materials. Renew. Sustain. Energy Rev. 16, 3065–3083.
Yap, H., Nixon, J., 2015. A multi-criteria analysis of options for energy recovery from municipal solid waste in India and the UK. Waste Manage. 46, 265–277.
Yin, C.-Y., 2011. Prediction of higher heating values of biomass from proximate and ultimate analyses. Fuel 90, 1128–1132.
You, H., Ma, Z., Tang, Y., Wang, Y., Yan, J., Ni, M., Cen, K., Huang, Q., 2017. Comparison of ANN (MLP), ANFIS, SVM, and RF models for the online classification of heating value of burning municipal solid waste in circulating fluidized bed incinerators. Waste Manage. 68, 186–197.
Zaman, A.U., 2010. Comparative study of municipal solid waste treatment technologies using life cycle assessment method. Int. J. Environ. Sci. Technol. 7, 225–234.
Zhao, R., Gupta, A., Novak, J.T., Goldsmith, C.D., Driskill, N., 2013. Characterization and treatment of organic constituents in landfill leachates that influence the UV disinfection in the publicly owned treatment works (POTWs). J. Hazard. Mater. 258, 1–9.